Optimal OFDM design for time-frequency dispersive channels

Thomas Strohmer and Scott Beaver

Abstract

Transmission over wireless channels is subject to time dispersion due to multipath propagation as well as frequency dispersion due to the Doppler effect. Standard OFDM systems using a guard time interval or cyclic prefix combat intersymbol interference but provide no protection against interchannel interference. This drawback has led to the introduction of pulse-shaping OFDM systems. In the first part of the paper we present a general framework for pulse shape design. Our analysis shows that certain pulse shapes proposed in the literature are in fact optimal in a well-defined sense. Furthermore our approach provides a simple way to adapt the pulse shape to varying channel conditions. In the second part of the paper we show that (pulse-shaping) OFDM systems based on rectangular time-frequency lattices are not optimal for time- and frequency dispersive wireless channels. This motivates the introduction of Lattice-OFDM (LOFDM) systems which are based on general time-frequency lattices. Using results from sphere packing theory we show how to optimally design LOFDM systems (the lattice and the pulse shape) for time- and frequency dispersive channels in order to minimize the joint ISI/ICI. Our theoretical analysis is confirmed by numerical simulations, showing that LOFDM systems outperform traditional pulse-shaping OFDM systems with respect to robustness against ISI/ICI.

Keywords

Interchannel interference, Intersymbol interference, Sphere packings, Pulse shaping, Orthogonal frequency division multiplexing.

I. Introduction

A. Problem statement

Orthogonal frequency division multiplexing (OFDM) is an efficient technology for wireless data transmission [1]. It is currently used in the European digital audio broadcasting standard [2], in digital terrestrial TV broadcasting, and broadband indoor wireless systems [3]. The advantages of OFDM include robustness against multipath fading and high spectral efficiency.

Transmission over wireless channels can lead to intersymbol interference (ISI) as well as interchannel interference (ICI). ISI is caused by time dispersion due to multipath propagation and ICI results from frequency dispersion due to the Doppler effect [4]. We will refer to channels that are time dispersive and frequency dispersive as *time-frequency dispersive*. The distortion resulting from time-frequency dispersive channels depends crucially on the time-frequency localization (TFL) of the pulse-shaping filter. For instance OFDM systems with guard-time interval or cyclic prefix can prevent ISI, but do not combat ICI, because they are based on rectangular-type pulses.

The authors are with the Department of Mathematics, University of California, Davis, CA-95616 USA. E-mail: strohmer@math.ucdavis.edu.

This work was partially supported by NSF grants 9973373 and 0208568.

The design of time-frequency well-localized pulse-shaping OFDM filters is therefore an active area of research [5], [6], [7], [8], [9]. Some of the proposed pulse shape design methods however involve the solution of highly non-linear optimization problems [6], [7], other approaches lead to pulse shapes that can be easily computed, but little or no theoretical justification of the optimality of the so-obtained pulse shapes has been given [5], [9], [8].

B. Our contributions

In the first part of this paper we present a general mathematical framework for pulse shape design for time-frequency dispersive channels. The features of our framework are: (i) it leads to pulse shapes that are optimally time-frequency localized in a well-defined mathematical sense; (ii) the pulse shapes can be easily computed numerically.

We note that the pulse shapes obtained by our approach have already been proposed to some extent in [5], [10], [9], [11], but except for some numerical observations in [5] no theoretical analysis about the optimality of these pulses has been given.

It is natural — and has been proposed frequently in the literature — that the time duration and the effective bandwidth of the pulse as well as the symbol period and the carrier separation of the OFDM system should be matched to the maximal delay spread and the maximal Doppler spread of the channel in order to minimize the joint ISI/ICI. The symbol period and the carrier separation define the time-frequency lattice associated with an OFDM system. All work on optimal OFDM design so far has exclusively dealt with rectangular time-frequency lattices. However such a setup is suboptimal for time-frequency dispersive channels, as we will show in the second part of the paper. By using results from sphere covering theory we demonstrate that OFDM systems constructed for hexagonal-type lattices provide better protection against ISI/ICI. To this end we introduce Lattice OFDM systems, which are OFDM systems based on general (non-rectangular) time-frequency lattices. We show that the pulse-shaping framework developed in Section III carries over to LOFDM systems. Furthermore we present a theoretical framework that leads to a simple method to optimally adapt the LOFDM system (i.e., the lattice and the pulse shape) to general time-frequency dispersive channels. Numerical simulations confirm our theoretical analysis, showing that LOFDM systems outperform OFDM systems. The improvement in the Signal-to-Noise-plus-Interference Ratio in our experiments was usually in the range of 1dB-2dB.

The paper is organized as follows. In the remaining part of this section we introduce some notation and some tools used frequently throughout the paper. In Section II we briefly review OFDM and discuss the difficulties posed by the vagaries of wireless channels. In Section III we present the aforementioned pulse-shaping framework. Section IV is devoted to the introduction of LOFDM, and the optimal design of LOFDM systems for given channel conditions. Numerical simulations in which we compare OFDM and LOFDM are presented in Section V. In Section VI we discuss some possible generalizations and open problems.

C. Preliminaries and Notation

We briefly review some basic concepts that we will need later. We also fix the notation used in this paper.

The Fourier transform of $f \in \boldsymbol{L}_2(\mathbb{R})$ denoted by $\hat{f}$ is

$$\hat{f}(\omega) = \int_{-\infty}^{+\infty} f(t) e^{-2\pi i t\omega} dt. \tag{1}$$

We also write $\mathcal{F}f$ instead of $\hat{f}$.

Let $f \in \boldsymbol{L}_2(\mathbb{R})$ and assume that the center of gravity of f is at $(0,0)$. As a measure of the "width" of f in time and frequency we shall often use the second-order moments

$$\Delta\tau_f = \int_{-\infty}^{+\infty} t^2 |f(t)|^2 dt, \qquad \Delta\nu_f = \int_{-\infty}^{+\infty} \nu^2 |\hat{f}(\nu)|^2 d\nu. \tag{2}$$

The *ambiguity function* of $f \in \boldsymbol{L}_2(\mathbb{R})$ is defined to be

$$Af(t,\omega) = \int_{-\infty}^{+\infty} f\big(x+\frac{t}{2}\big)\overline{f\big(x-\frac{t}{2}\big)} e^{-2\pi i\omega x} dx, \tag{3}$$

where $\overline{f(t)}$ denotes the conjugate of $f(t)$. The *cross-ambiguity function* of f and $g \in \boldsymbol{L}_2(\mathbb{R})$ is

$$A(f,g)(t,\omega) = \int_{-\infty}^{+\infty} f\big(x+\frac{t}{2}\big)\overline{g\big(x-\frac{t}{2}\big)} e^{-2\pi i\omega x} dx. \tag{4}$$

For our analysis we are mainly interested in $|Af|^2$ and $|A(f,g)|^2$ rather than the ambiguity function itself. Therefore we could equally well use the Wigner distribution or the Short time Fourier transform.

We define the dilation operator $\mathcal{D}_\alpha$ by

$$\mathcal{D}_\alpha f(t) = \sqrt{\alpha} f(\alpha t), \qquad \alpha \in \mathbb{R}^+, \tag{5}$$

and the multiplication by a chirp is

$$\mathcal{C}_\beta f(t) = f(t) e^{-\pi i\beta t^2}, \qquad \beta \in \mathbb{R}. \tag{6}$$

$\mathcal{D}_\alpha$ and $\mathcal{C}_\beta$ are unitary operators, and we have $\mathcal{D}_\alpha^{-1} = \mathcal{D}_{\alpha^{-1}}$ and $\mathcal{C}_\beta^{-1} = \mathcal{C}_{-\beta}$.

For $f, h \in \boldsymbol{L}_2(\mathbb{R})$ we have [12]

$$A(\mathcal{D}_\alpha f, \mathcal{D}_\alpha h)(t,\omega) = A(f,h)(\alpha t, \alpha^{-1}\omega) \tag{7}$$
$$A(\mathcal{C}_\beta f, \mathcal{C}_\beta h)(t,\omega) = A(f,h)(t, \omega + \beta t). \tag{8}$$

If not otherwise specified norms of functions and sequences will always be $\boldsymbol{L}^2$-norms and $\boldsymbol{\ell}^2$-norms respectively, i.e., for a function $f \in \boldsymbol{L}_2(\mathbb{R})$ we have

$$\|f\| = \left(\int_{-\infty}^{+\infty} |f(t)|^2 \, dt \right)^{\frac{1}{2}},$$

and for a sequence $x = \{x_k\}_{k\in\mathbb{Z}} \in \boldsymbol{\ell}_2(\mathbb{Z})$ we have

$$\|x\| = \left(\sum_{k\in\mathbb{Z}} |x_k|^2 \right)^{\frac{1}{2}}.$$

A sequence of functions $\{f_k\}_{k\in\mathbb{Z}}$ is called a Riesz basis for a (separable) Hilbert space[1] $\mathcal{H}$ if $\{f_k\}_{k\in\mathbb{Z}}$ is complete in $\mathcal{H}$ and there exist constants $C_1, C_2 > 0$ such that for every $n \in \mathbb{N}$ and every sequence $c_0, , \dots, c_{n-1}$ of scalars one has

$$C_1 \sum_{k=0}^{n-1} |c_k|^2 \le \Big\| \sum_{k=0}^{n-1} c_k f_k \Big\|^2 \le C_2 \sum_{k=0}^{n-1} |c_k|^2, \tag{9}$$

see [13]. The Gram matrix R associated with the Riesz basis $\{f_k\}_{k\in\mathbb{Z}}$ has the entries $R_{k,l} = \langle f_l, f_k \rangle$, $k, l \in \mathbb{Z}$, and satisfies $C_1 I \le R \le C_2 I$, where I is the identity operator on $\boldsymbol{\ell}_2(\mathbb{Z})$.[2] For any Riesz basis $\{f_k\}_{k\in\mathbb{Z}}$ there exists a unique *dual* Riesz basis $\{h_k\}_{k\in\mathbb{Z}}$, such that $\{f_k\}_{k\in\mathbb{Z}}$ and $\{h_k\}_{k\in\mathbb{Z}}$ are *biorthogonal*, i.e.,

$$\langle f_k, h_l \rangle = \delta_{k,l}, \qquad k, l \in \mathbb{Z},$$

where $\delta_{k,l}$ denotes the Kronecker delta.

II. OFDM, wireless channels, and time-frequency localization

Let us briefly review the basic scheme of OFDM. The transmission functions of an orthogonal frequency division multiplexing (OFDM) system consist of translations and modulations of a single pulse shape φ, i.e.,

$$\varphi_{kl}(t) = \varphi(t - kT) e^{2\pi i l F t}, \tag{10}$$

[1]In a nutshell, a Hilbert space is a vector space equipped with an inner product $\langle\cdot,\cdot\rangle$ and a norm given by $\|\cdot\| = \sqrt{\langle\cdot,\cdot\rangle}$.
[2]For positive definite operators R and S, we say $R > S$ if $\langle Rx, x\rangle > \langle Sx, x\rangle$ for all $x \neq 0$.

for some $T, F > 0, k, \in \mathbb{Z}$ and $l = 0, \ldots, N-1$ or $l \in \mathbb{Z}$. We denote such a function system generated via (10) by the triple (φ, T, F), whether or not the functions are orthogonal.

Here T is the symbol period and F is the carrier separation. Let W be the given bandwidth, then $N = W/F$ is the number of subcarriers. Throughout our analysis it is convenient to assume an infinite number of subcarriers. Thus the frequency index l in (10) runs through the set of integers instead of from 0 to $N-1$. But many of the results presented in this paper also hold for finitely many subcarriers, either verbatim or with a negligible approximation error.

A necessary condition for perfect reconstruction of the data is that the functions $\varphi_{k,l}$ are linearly independent (no matter if they are orthogonal or not). This implies that $TF \geq 1$, which follows easily from the connection between OFDM systems and Gabor frames, e.g., see [8] or the appendix. We note that orthogonality of the functions $\varphi_{k,l}$ is not a requirement for perfect reconstruction, but minimizes the error caused by AWGN.

As shown in [7] for a large number of subcarriers the *spectral efficiency* ρ of the OFDM system in terms of data symbols per second per Hertz is approximately given by $\rho = (TF)^{-1}$. Since $TF \geq 1$ we have of course that the maximal spectral efficiency is $\rho_{\max} = 1$.

Let $c_{k,l}, k \in \mathbb{Z}, l = 0, \ldots N-1$ be the (already block-coded) data symbols to be transmitted. The OFDM signal is then given by

$$s(t) = \sum_{k,l} c_{k,l} \varphi_{k,l}. \tag{11}$$

The received signal is

$$r(t) = (\mathbf{H}s)(t) + \varepsilon(t) = \int_{-\infty}^{+\infty} h(t, \tau) s(t - \tau) d\tau + \varepsilon(t), \tag{12}$$

where $h(t, \tau)$ is the impulse response of the time-varying channel $\mathbf{H}$ [14] and $\varepsilon(t)$ is zero-mean stationary white noise. The data symbol $c_{k,l}$ is transmitted at the (k, l)-th lattice point of the rectangular time-frequency lattice $(kT, lF), k, l \in \mathbb{Z}$.

Assuming that the $\varphi_{k,l}$ are orthonormal the transmitted data are recovered by computing the inner product of the received signal r with the functions $\varphi_{k,l}$, i.e., $\tilde{c}_{k,l} = \langle r, \varphi_{k,l} \rangle$. By (11) and (12) we have

$$\tilde{c}_{k,l} = \langle \mathbf{H}s, \varphi_{k,l} \rangle + \langle \varepsilon, \varphi_{k,l} \rangle = \sum_{k',l'} c_{k',l'} \langle \mathbf{H}\varphi_{k',l'}, \varphi_{k,l} \rangle + \langle \varepsilon, \varphi_{k,l} \rangle, \tag{13}$$

where the interchange of summation and integration is justified under mild smoothness and decay conditions on φ and $\mathbf{H}$. In the ideal (but unrealistic) case the wireless channel does not introduce any distortion. Thus the orthogonality between the functions $\psi_{k,l}$ is preserved, and if $\varepsilon = 0$ the data $c_{k,l}$ can be recovered exactly. However in practice wireless channels are time-dispersive and frequency-dispersive. Hence when $\varphi_{k,l}$ passes through the time-varying channel $\mathbf{H}$ it is spread out in time and frequency, causing ISI as well as ICI in the transmitted data. It is customary (cf. e.g. [5], [4], [7], [8]) to describe the channel by the *maximal excess delay* τ_0 and the *maximal Doppler spread* ν_0 of the channel scattering function.

It is clear from (13) that the interference of the data symbol $c_{k,l}$ with neighbor symbols will be smaller with better time-frequency localization of $\varphi_{k,l}$ and with larger distance between $c_{k,l}$ and adjacent data symbols in the time-frequency domain, i.e, the larger T and F. The latter condition however comes at the cost of reduced spectral efficiency.

Ideally we would like to construct an OFDM system (φ, T, F) that satisfies the following three requirements simultaneously:
(i) the functions $\psi_{k,l}$ are mutually orthogonal,
(ii) φ is well-localized in time and frequency domain,
(iii) $TF = 1$, i.e., maximal spectral efficiency.

As is well-known from Gabor theory these three conditions cannot be satisfied simultaneously due to the Balian-Low Theorem [15] (see the appendix for a brief discussion of the connection between OFDM and Gabor systems). This holds true, even if we relax condition (i) and consider biorthogonality instead (which however would increase the sensitivity of the system to AWGN).

Hence we relax condition (iii) and allow $TF > 1$. This loss in spectral efficiency is usually an acceptable price to pay to mitigate ISI/ICI (as long as TF is not too large)[3].

III. A general framework for pulse shape design

As pointed out above in a dispersive channel the transmitted signal is spread in time and in frequency, causing ISI and ICI. This interference can be reduced if the pulse shape is well-localized in time and frequency. The classical way to measure the time- and frequency localization involves the Heisenberg Uncertainty Principle. More precisely, if $f \in \boldsymbol{L}_2(\mathbb{R})$ and $\tau, \omega \in \mathbb{R}$ are arbitrary,

$$\left(\int_{-\infty}^{+\infty} (t-\tau)^2 |f(t)|^2 dt\right)^{\frac{1}{2}} \left(\int_{-\infty}^{+\infty} (\nu-\omega)^2 |\hat{f}(\nu)|^2 d\nu\right)^{\frac{1}{2}} \geq \frac{\|f\|^2}{4\pi}. \tag{14}$$

Equality holds if and only if f is of the form $f(t) = ce^{2\pi i\omega(t-\tau)}e^{-\pi\alpha(t-\tau)^2}$ for $\tau, \omega \in \mathbb{R}, c \neq 0$, and $\alpha > 0$, i.e., if f is a (possibly translated, modulated, dilated) Gaussian.

In (14) time and frequency are treated separately. It seems more appropriate in our context — in particular with respect to time-frequency dispersive channels — to measure the TFL by considering time and frequency simultaneously. Moreover in light of (13) we are naturally interested in measuring the cross interference between different transmitter functions $\varphi_{k,l}$ and $\varphi_{k',l'}$. Thus we replace the pair $(f, \hat{f})$ by a joint time-frequency representation of two functions f and h, such as the cross ambiguity function $A(f, h)$.

In light of the Heisenberg Uncertainty Principle it is not surprising that $A(f, h)$ cannot be arbitrarily well concentrated. This can be expressed for instance by the fact that $A(f, h)$ cannot be compactly supported, see [16]. An alternative formulation is the following Heisenberg-type inequality [17], [18].

[3] Alternatively we can use a slightly different modulation scheme, known as OQAM-OFDM, see [6]. A comparison between these two approaches is beyond the scope of this paper.

Theorem III.1: For every $f, h \in \boldsymbol{L}_2(\mathbb{R})$ there holds

$$\int_{-\infty}^{+\infty}\int_{-\infty}^{+\infty} (t-\tau)^2 |A(f,h)(t,\nu)|^2 dt\, d\nu \cdot \int_{-\infty}^{+\infty}\int_{-\infty}^{+\infty} (\nu-\omega)^2 |A(f,h)(t,\nu)|^2 dt\, d\nu \geq \frac{\|f\|^4 \|h\|^4}{4\pi^2}. \tag{15}$$

Equality holds if and only if

$$\begin{aligned} f(t) &= c_1 e^{2\pi i \beta t} e^{-\pi\alpha(t-s)^2}, \\ h(t) &= c_2 e^{2\pi i (\omega+\beta) t} e^{-\pi\alpha(t-\tau-s)^2}, \end{aligned} \tag{16}$$

with $\alpha > 0, c_1, c_2 \neq 0$, and $\beta, s, \tau \in \mathbb{R}$.

Thus again, translated, modulated, and dilated versions of the Gaussian lead to optimal time-frequency localization.

¿From now on we will always denote Gaussians by g^σ, i.e.,

$$g^\sigma(t) := (2\sigma)^{1/4} e^{-\pi\sigma t^2}. \tag{17}$$

If $\sigma = 1$ we skip the superscript and simply write g instead. Since the Gaussian itself obviously does not yield an orthogonal set of transmission functions $g^\sigma_{k,l}$ as defined via (10)[4], we use a standard method to "orthogonalize" the set $\{g_{k,l}\}$. In connection with pulse shape design it has been used implicitly in [5] (see also [19]), and explicitly in [10], [9], [11].

In general this procedure can be described as follows. Given a function f with "nice" decay and assume that (f, T, F) is linearly independent. We can construct an orthonormal system (φ, T, F) from (f, T, F) via[5]

$$\varphi = \sum_{k,l} R^{-\frac{1}{2}}_{k,l,0,0} f_{k,l}, \tag{18}$$

where

$$R_{k,l,k',l'} = \langle f_{k',l'}, f_{k,l} \rangle. \tag{19}$$

We will write

$$\varphi = \mathrm{orth}(f, T, F) \tag{20}$$

for this procedure.

[4]Since $g^\sigma(t) > 0$ for all t, $g^\sigma(t)$ can never by orthogonal to any of its shifted copies, a similar argument holds of course for g^σ and its modulations.

[5]The existence of $R^{-\frac{1}{2}}$ follows from the positive-definiteness of R, which in turn follows from the assumption that (f, T, F) is linear independent.

For $f = g^\sigma$ the linear independence of (g^σ, T, F) follows from the fact that $(g^\sigma, 1/F, 1/T)$ is a frame for $TF > 1$, see the Appendix for more details. Since the pulse shape obtained from the Gaussian via (20) plays a major role throughout the paper we introduce a separate notation for this pulse to distinguish it from general OFDM pulses. We denote

$$\psi^\sigma := \operatorname{orth}(g^\sigma, T, F), \tag{21}$$

and if $\sigma = 1$ we skip the superscript and simply write ψ.

The following theorem shows that the orthogonalization procedure described above yields pulse shapes that are optimal in a certain sense.

Theorem III.2: Let $\{f_{k,l}\}$ with $f_{k,l}(t) = f(t - kT)e^{2\pi i l F t}$ and $\|f\| = 1$ be a Riesz basis for the separable Hilbert space $\mathcal{H}$.
(i) The function $\varphi_{\text{opt}} = \operatorname{orth}(f, T, F)$ is optimally close to f in the sense that φ_{opt} solves the optimization problem

$$\arg\min_{\varphi} \|Af - A\varphi\|_2 \qquad \text{subject to } (\varphi, T, F) \text{ is an orthonormal basis for } \mathcal{H}. \tag{22}$$

(ii) Furthermore

$$\|Af - A\varphi_{\text{opt}}\| \le \max\{|1 - \theta_{\min}^{-\frac{1}{2}}|^2, |1 - \theta_{\max}^{-\frac{1}{2}}|^2\}, \tag{23}$$

where $\theta_{\min}$ and $\theta_{\max}$ are the minimal and maximal eigenvalues respectively of R.

The proof is given in the Appendix. Theorems III.1 and III.2 imply that the OFDM pulse shapes $\psi^\sigma = \operatorname{orth}(g^\sigma, T, F)$ are optimally time-frequency localized among all possible OFDM pulse shapes in the sense that they are closest (in the $\boldsymbol{L}^2$-sense) to the Gaussian g^σ. Unlike g^σ we see from Example 2 in Section 6 of [19] that ψ^σ has "only" exponential decay in time and frequency. Here the constant in the exponent depends on the condition number of $R(g^\sigma, T, F)$. In Figure 1 we display the behavior of $\operatorname{cond}(R(g^\sigma, T, F))$ in dependence of the spectral efficiency $(TF)^{-1}$ for $(TF)^{-1} = \frac{p}{p+1}$ with $p = 1, 2, \dots, 25$. When $(TF)^{-1} \to 1$ we have $\operatorname{cond}(R(g^\sigma, T, F)) \to \infty$ as a consequence of the Balian-Low Theorem and the functions ψ^σ become increasingly ill-localized, cf. also Theorem 7.3 in [20]. Fortunately for typical values of $(TF)^{-1}$ in OFDM such as $TF \in [\frac{1}{2}, \frac{4}{5}]$ (and $\sigma = F/T$) the condition number of R is small. For instance for $TF = 2$ one can show analytically [21] that $\operatorname{cond}(R(g^\sigma, T/\sqrt{\sigma}, 2\sqrt{\sigma}/T)) = \sqrt{2}$ and for $TF = \frac{3}{2}$ a numerical inspection yields $\operatorname{cond}(R(g^\sigma, T/\sqrt{\sigma}, \frac{3}{2}\sqrt{\sigma}/T)) = \sqrt{3}$. The second graph in Figure 1 corresponds to the condition number of the Gram matrix of a modified OFDM system, which we will introduce in the next section.

For a general theoretical investigation of the decay properties of pulse shapes generated via (20) we refer to [11]. Efficient numerical algorithms to compute ψ^σ that are also applicable if $TF \neq \mathbb{N}$ can be easily derived from the algorithms in [22].

It has been shown in [19] that for certain pulse shapes the so-called IOTA approach in [5] is equivalent to (20). In [5] the authors computed numerically the TFL of ψ via (14) as $(\Delta\tau_\psi \cdot \Delta\nu_\psi)^{-1} = 0.977 \cdot 4\pi$ (as compared to 4π for the Gaussian) and conjectured that this is the optimal value for all pulse shapes that create an OFDM system with spectral efficiency $\frac{1}{2}$. Theorem III.2 provides additional evidence for the correctness of their conjecture (as long as we consider only rectangular time-frequency lattices).

In order to reduce ISI and ICI it often has been suggested to choose the time duration $\Delta\tau_f$ and the frequency duration $\Delta\nu_f$ of the transmission pulse as well as the parameters F and T such that they are adapted to the channel properties, cf. e.g. [5], [7], [8] and for a more theoretical approach see [23]. This means that for given maximal excess delay τ_0 and maximal Doppler spread ν_0 we choose $\Delta\tau_f$, $\Delta\nu_f$, T, and F such that

$$\frac{\tau_0}{\nu_0} \approx \frac{\Delta\tau_f}{\Delta\nu_f} \approx \frac{T}{F}. \tag{24}$$

For the Gaussian-based window ψ^σ this means we set $\sigma \approx \frac{\nu_0}{\tau_0}$ and $T = \sqrt{\frac{1}{\sigma\rho}}$, $F = \sqrt{\frac{\sigma}{\rho}}$ for given spectral efficiency ρ. Using basic properties of the dilation operator $\mathcal{D}_\alpha$ we obtain the relation

$$\psi^\sigma = \operatorname{orth}(g^\sigma, 1/\sqrt{\sigma\rho}, \sqrt{\sigma/\rho}) = \mathcal{D}_{\sqrt{\sigma}}\big(\operatorname{orth}(g, 1/\sqrt{\rho}, 1/\sqrt{\rho})\big) = \mathcal{D}_{\sqrt{\sigma}}\psi. \tag{25}$$

Thus the transmission pulse ψ^σ that is matched to the channel parameters τ_0 and ν_0 is obtained from the "standard" pulse ψ by an appropriate dilation.

Hence at least theoretically it is very easy to adapt the OFDM system to time-varying channel conditions. We only have to know how the ratio of τ_0 and ν_0 changes and adapt the lattice and ψ^σ accordingly by a simple dilation. Of course, in practice we also have to deal with issues such as time and frequency synchronization when we change the lattice parameters, which may be a non-trivial task.

IV. Lattice-OFDM, wireless channels, and interference

The robustness of an OFDM system against ISI and ICI depends essentially on two factors:

(i) The time-frequency localization of ψ_{kl};

(ii) the distance between adjacent time-frequency lattice points (kT, lF), $((k \pm 1)T, ((l \pm 1)F)$.

We have seen in the previous section how to construct for given channel conditions OFDM pulse shapes with optimal time-frequency concentration. If we want to further improve the stability of the OFDM system against interference we have to increase the distance between adjacent data symbols by increasing the distance between adjacent grid points. However increasing T and/or F results in an undesirable loss of spectral efficiency. Hence we are concerned with the following question: *Can we increase the distance between adjacent grid points without reducing the spectral efficiency?*

We will show in this section that this is indeed possible. The solution lies in the introduction of a more general and flexible OFDM setup which we call *Lattice-OFDM* (LOFDM).

A. Lattice-OFDM

We briefly review some basic facts about lattices, see [24] for details. Any lattice Λ can be described by its (non-unique) generator matrix L. The generator matrix contains the coordinates of the column-vectors that describe the fundamental domain of a lattice. The density $\delta(\Lambda)$ of the lattice Λ is given by

$$\delta(\Lambda) = \frac{1}{\det(L)}. \tag{26}$$

For instance the generator matrix L_R for the rectangular lattice Λ_R displayed in Figure 2 is

$$L_R = \begin{bmatrix} T & 0 \\ 0 & F \end{bmatrix}, \tag{27}$$

the density of Λ_R is $\delta(\Lambda_R) = 1/\det(L_R) = 1/(TF)$. The hexagonal lattice Λ_H (shown in Figure 3 with $T = F$) with generator matrix

$$L_H = \begin{bmatrix} \frac{\sqrt{2}}{\sqrt[4]{3}}T & \frac{\sqrt{2}}{2\sqrt[4]{3}}T \\ 0 & \frac{\sqrt[4]{3}}{\sqrt{2}}F \end{bmatrix} \tag{28}$$

has the same density, viz. $\delta(\Lambda_H) = 1/\det(L_H) = 1/(TF)$.

Definition IV.1: Let Λ be a lattice with generator matrix

$$L = \begin{bmatrix} x & y \\ 0 & z \end{bmatrix}, \qquad x, z \neq 0, \tag{29}$$

and let $\varphi \in \boldsymbol{L}_2(\mathbb{R})$ be given. We denote by (φ, Λ) the function system

$$\varphi_{k,l}(t) = \varphi(t - \lambda_k)e^{2\pi i \mu_l t}, \qquad (\lambda_k, \mu_l) \in \Lambda, \quad k \in \mathbb{Z},\, l = 0, \ldots, N-1 \text{ or } l \in \mathbb{Z}. \tag{30}$$

If the functions $\varphi_{k,l}$ are mutually orthonormal we call (φ, Λ) a Lattice-OFDM (LOFDM) system. Furthermore the Gram matrix $R(\varphi, \Lambda)$ associated with (φ, Λ) is defined via

$$R(\varphi, \Lambda) := \{R_{k,l,k',l'}\} \quad \text{with } R_{k,l,k',l'} = \langle \varphi_{k',l'}, \varphi_{k,l} \rangle. \tag{31}$$

It is clear that the spectral efficiency ρ of an LOFDM system (ψ, Λ) coincides with the density of the lattice. i.e., $\rho = 1/\det(L)$.

Note: We have restricted in the definition of LOFDM to lattices with upper-triangular generator matrices, instead of general invertible 2×2 generator matrices. The reason is that unlike general lattices those with upper-triangular generator matrix — though not necessarily separable — still possess a distinctive orientation along the time-axis and the frequency-axis respectively. This orientation is very useful for an efficient numerical implementation (see also Section V) and it keeps the time delay introduced by the non-separability of the lattice small. All results that follow could be derived (with some minor adaptations) for general lattices, however with little or no practical benefit.

B. Sphere packings and minimization of ISI/ICI

In this section we show how to design pulse shapes and lattices which provide optimal robustness for time-frequency dispersive channels. We start with a specific but important example. The analysis of the general case will be based on this example.

Assume that the parameters of the channel scattering function satisfy $\tau_0 = \nu_0$ (we will discuss more general choices for τ_0, ν_0 later). By the results in Section III the optimal pulse shape ψ in this case is given by $\psi = \text{orth}(g, T, F)$ with $g(t) = 2^{\frac{1}{4}} e^{-\pi t^2}$ (since $\sigma = \frac{\nu_0}{\tau_0} = 1$) and $T = F$.

For a function f and $\varepsilon > 0$ define the *effective support* of the ambiguity function Af by

$$\text{supp}_\varepsilon(Af) = \{(t, \omega) : |Af(t, \omega)| > \varepsilon\}. \tag{32}$$

The ambiguity function of g is rotation-invariant, see [25], therefore $|Ag_{k,l}|$ is rotation invariant. Hence for any $\varepsilon > 0$, $\text{supp}_\varepsilon(Ag_{k,l})$ is a sphere with center (kT, lF). It follows from (23) that if the matrix R is well-conditioned then $A\psi \approx Ag$. Hence $\text{supp}_\varepsilon(A\psi_{k,l})$ is approximately a sphere with center (kT, lF). The OFDM system (ψ, T, F) with $T = F$ and $\sigma = 1$ can thus be represented schematically by Figure 2. The data symbol $c_{k,l}$ is transmitted at the lattice point (kT, lF). The gray spheres represent $\text{supp}_\varepsilon A\psi_{k,l}$. We have chosen ε such that the difference between the setup in Figure 2 and Figure 3, see below, becomes obvious. The reader should not be confused by the fact that the spheres may overlap for smaller ε. The $A\psi_{k,l}$ are of course mutually orthogonal, since the $\psi_{k,l}$ are mutually orthogonal. However after passing through the channel $\mathbf{H}$ the orthogonality between the $\psi_{k,l}$ (and thus between the $A\psi_{k,l}$) is lost and the support of $A\psi_{k,l}$ is spread out in time and frequency. And now the overlap between adjacent $A\psi_{k,l}$'s (or rather between $A\mathbf{H}\psi_{k,l}$ and $A\mathbf{H}\psi_{k',l'}$) plays a crucial role. Roughly speaking less overlap between the spheres results in less ISI and ICI.

Note that since $\psi_{k,l}(t) = \mathcal{O}(e^{-|t|})$ we have

$$|\langle \mathbf{H}\psi_{k,l}, \psi_{k\pm1,l\pm1}\rangle| \gg |\langle \mathbf{H}\psi_{k,l}, \psi_{k\pm n,l\pm n}\rangle|, \quad \text{for } n > 1. \tag{33}$$

Therefore we can concentrate on the interference between $c_{k,l}$ and direct neighbor symbols $c_{k\pm1,l\pm1}$, since the interference of $c_{k,l}$ with symbols $c_{k\pm n,l\pm n}$ where $n > 1$ will be negligibly small by comparison.

Hence the problem reduces to maximizing the distance between immediate neighbor lattice points (k, l) and $(k \pm 1, l \pm 1)$ without losing spectral efficiency. The answer to this problem comes from the theory of sphere packings.

The sphere packing problem can be loosely described as follows. We are given an infinite number of d-dimensional spheres of equal size. We identify the midpoint of each sphere with a point of a d-dimensional lattice Λ in $\mathbb{R}^d$. In the sphere packing problem one tries to find the lattice Λ_{opt} that solves

$$\max_{\Lambda} \left\{ \frac{\text{Volume of a sphere}}{\text{Density of } \Lambda} \right\}. \tag{34}$$

It is easy to see that in the sphere packing problem the radius r of a sphere is given by

$$r = \frac{1}{2}\Big(\min_{\substack{\lambda_k,\, \lambda_l \in \Lambda,\\ \lambda_k \neq \lambda_l}} \big\{\|\lambda_k - \lambda_l\|\big\}\Big). \tag{35}$$

In words, the radius is equal to half of the minimal distance between two lattice points. We can reformulate (34) as follows:

$$\max_{\Lambda}\Big(\min_{\substack{\lambda_k,\, \lambda_l \in \Lambda,\\ \lambda_k \neq \lambda_l}} \big\{\|\lambda_k - \lambda_l\|\big\}\Big) \qquad \text{subject to } \delta(\Lambda) = \delta_0, \tag{36}$$

for some arbitrary $\delta_0 > 0$.

Obviously we find ourselves confronted with the same problem as in OFDM, when we want to maximize the distance between adjacent lattice points in order to minimize ISI/ICI while keeping the spectral efficiency constant.

It is well-known that the sphere packing problem in 2-d is solved by the hexagonal lattice, cf. [24]. Thus for the case $\tau_0 = \nu_0$ an OFDM system constructed from a hexagonal lattice as shown in Figure 3 will provide optimal protection against ISI/ICI due to the increased distance between adjacent lattice points.

The effect of the increased distance becomes apparent when comparing Figure 2 with Figure 3. In both cases we have chosen the same ε as threshold for the effective support of the ambiguity function.

Furthermore when we construct an orthogonal set of transmission functions (ψ, Λ) from a non-orthogonal set of Gaussians (g^σ, Λ) via $\psi = \mathrm{orth}(\varphi, \Lambda)$ the increased distance between adjacent lattice points yields a smaller correlation $|\langle g^\sigma_{k,l}, g^\sigma_{k',l'}\rangle|$ between "adjacent" functions than in the case of a rectangular lattice. This results in a smaller condition number of the associated Gram matrix $R(g^\sigma, \Lambda)$ for $R(g^\sigma, T, F)$ at the same spectral efficiency, as can be seen in Figure 1.

Of course the assumption $\tau_0 = \nu_0$ in our example is very restrictive. In the next subsection we consider more general channel conditions and derive a general LOFDM design rule in order to minimize the joint ISI/ICI.

C. Optimal LOFDM design for the minimization of ISI/ICI

Recall that τ_0 and ν_0 describe the support of the channel scattering function. More precisely, assuming that the support of the scattering function is circumscribed by a rectangle (or ellipse), then τ_0 gives the length of the rectangle (in the time-direction) and ν_0 corresponds to the width (in the frequency direction). In the following we extend the result from the previous section to more general (and more realistic) choices for τ_0 and ν_0. In fact our approach will also include the case where the support of the scattering function may be concentrated along a rotated rectangle in the time-frequency domain (like a chirp). Such a setup has also been investigated in [26].

The next theorem is the key to extending the optimal LOFDM setup derived for the special case $\tau_0 = \nu_0$ to the general case. It shows how we can switch between different lattices by adapting the pulse shape accordingly in order to preserve the properties of the optimal "hexagonal" case. The theorem is essentially only a special case of a deep theorem by Gröchenig [12].

Theorem IV.2: Let (f_1, Λ_1) be a non-orthogonal, linear independent system with $\|R(f_1, \Lambda_1)\| < \infty$ and denote $\varphi_1 = \operatorname{orth}(f_1, \Lambda_1)$. Assume Λ_2 is a lattice with density $\delta(\Lambda_2) = \delta(\Lambda_1)$ and let

$$L_1 = \begin{bmatrix} x_1 & y_1 \\ 0 & z_1 \end{bmatrix}, \qquad L_2 = \begin{bmatrix} x_2 & y_2 \\ 0 & z_2 \end{bmatrix} \tag{37}$$

be the generator matrices of Λ_1 and Λ_2 respectively. If

$$f_2 = \mathcal{F}\mathcal{D}_{\alpha^{-1}}\mathcal{C}_{-\beta\alpha^2}\mathcal{F}^{-1}f_1 \tag{38}$$

with

$$\alpha = \frac{z_2}{z_1}, \quad \beta = -\frac{y_2}{z_2} + \frac{y_1}{z_1}\frac{{z_1}^2}{{z_2}^2}, \tag{39}$$

then

$$R(f_2, \Lambda_2) = R(f_1, \Lambda_1). \tag{40}$$

Furthermore define $\varphi_2 = \operatorname{orth}(f_2, \Lambda_2)$, then

$$\varphi_2 = \mathcal{F}\mathcal{D}_{\alpha^{-1}}\mathcal{C}_{-\beta\alpha^2}\mathcal{F}^{-1}\varphi_1. \tag{41}$$

Proof: The proof consists of applying twice Proposition 9.4.4 in [12].

To see this we choose an arbitrary rectangular lattice Λ_R with generator matrix

$$L_R = \begin{bmatrix} T & 0 \\ 0 & F \end{bmatrix} \tag{42}$$

such that $\delta(\Lambda_R) = \delta(\Lambda_1)$. One readily verifies by inspection that L_1 and L_2 can be written as

$$L_1 = JC_{\beta_1}D_{\alpha_1}J^{-1}L_R, \qquad \text{with } \alpha_1 = \frac{z_1}{F}, \beta_1 = -\frac{y_1}{z_1}, \tag{43}$$

$$L_2 = JC_{\beta_2}D_{\alpha_2}J^{-1}L_R, \qquad \text{with } \alpha_2 = \frac{z_2}{F}, \beta_2 = -\frac{y_2}{z_2}, \tag{44}$$

where J, C_β, D_α are defined by

$$J = \begin{bmatrix} 0 & -1 \\ 1 & 0 \end{bmatrix}, \quad C_\beta = \begin{bmatrix} 1 & 0 \\ \beta & 1 \end{bmatrix}, \quad D_\alpha = \begin{bmatrix} \alpha & 0 \\ 0 & \alpha^{-1} \end{bmatrix}, \quad \alpha, \beta \in \mathbb{R}. \tag{45}$$

Let $\operatorname{Sp}(d, \mathbb{R})$ denote the symplectic group (the expression $(d, \mathbb{R})$ specifies that we are dealing with $2d \times 2d$ real-valued matrices). Let $\mu(\cdot)$ denote the symplectic (unitary) operator appearing in the metaplectic representation of $\mathrm{Sp}(d,\mathbb{R})$, cf. [25, Chapter 4]. Of the many deep properties of $\mu(\cdot)$ we only need the following ones. Let J, C_β, D_α be as defined in (45), then

$$\mu(J) = \mathcal{F}^{-1}, \quad \mu(C_\beta) = \mathcal{C}_{-\beta}, \quad \mu(D_\alpha) = \mathcal{D}_{\alpha^{-1}}, \tag{46}$$

where $\mathcal{F}, \mathcal{C}, \mathcal{D}$ are as defined in (1), (5) and (6) respectively. Furthermore there holds

$$\mu(JCDJ^{-1}) = \mu(J)\mu(C)\mu(D)\mu(J^{-1}). \tag{47}$$

Since $J, C_\beta, D_\alpha \in \mathrm{Sp}(1,\mathbb{R})$ it follows that[6]

$$A_1 := JC_{\beta_1}D_{\alpha_1}J^{-1} \in \mathrm{Sp}(1,\mathbb{R}), \quad A_2 := JC_{\beta_2}D_{\alpha_2}J^{-1} \in \mathrm{Sp}(1,\mathbb{R}). \tag{48}$$

Set $f_R = \mu(A_1)^{-1}f_1$ and $f_2 = \mu(A_2)f_R$. It follows from Proposition 9.4.4 in [12] that

$$(f_R, \Lambda_R) = \mu(A_1)^{-1}(f_1, \Lambda_1), \tag{49}$$

and

$$(f_2, \Lambda_2) = \mu(A_2)(f_R, \Lambda_R). \tag{50}$$

Since $\mu(A_1)$ and $\mu(A_2)$ are unitary operators we get $R(f_1,\Lambda_1) = R(f_R,\Lambda_R) = R(f_2,\Lambda_2)$ where $f_2 = \mu(A_2)\mu(A_1)^{-1}f_1$ and $L_2 = A_2A_1^{-1}L_1$. Hence it remains to check that $\mu(A_2)\mu(A_1)^{-1}f_1$ is indeed of the form (38)–(39) as assumed. Using (43)– (45) and (47) we get after a simple calculation

$$\mu(A_2)\mu(A_1)^{-1} = \mu(JC_\beta D_\alpha J^{-1}) \tag{51}$$

where α and β are as defined in (39). Using relations (46) and the fact that $C_\beta D_\alpha = D_\alpha C_{\beta\alpha^2}$ we obtain

$$f_2 = \mu(A_2)\mu(A_1)^{-1}f_1 = \mathcal{F}\mathcal{D}_{\alpha^{-1}}C_{-\beta\alpha^2}\mathcal{F}^{-1}f_1. \tag{52}$$

Equation (41) follows now from (38) and (40). ❑

Remark: The pulse-shaping framework derived in Section III also holds for general lattices, since Theorem III.2 carries over to general lattices. The proof of the extension of Theorem III.2 can be done by using Theorem IV.2 and the results derived in Chapter 9.4 in [12].

It is possible to prove Theorem IV.2 directly using signal analytic methods. However we feel that the metaplectic representation is simpler and more elegant. The reader familiar with the mathematical theory of quantum physics will notice that Theorem IV.2 is essentially a consequence of the celebrated Stone-von Neumann Theorem on unitary representations of the Heisenberg group.

The main feature of Theorem IV.2 is of course that it yields a simple rule for the design of optimal LOFDM systems for time-frequency dispersive channels. We will illustrate this fact by some examples.

[6] In fact, any lattice in $\mathbb{R}^{2d}$ has a generator matrix which belongs to $\mathrm{Sp}(1,\mathbb{R})$

D. Some examples

In the following examples we consider LOFDM systems with spectral efficiency ρ. In this subsection Λ_1 will denote the hexagonal lattice Λ_H with generator matrix

$$L_H = L_1 = \begin{bmatrix} \frac{\sqrt{2}}{\sqrt[4]{3}\sqrt{\rho}} & \frac{1}{\sqrt[4]{3}} \\ 0 & \frac{\sqrt[4]{3}}{\sqrt{2}\sqrt{\rho}} \end{bmatrix} \tag{53}$$

and

$$\varphi_1 = \psi = \mathrm{orth}(g, \Lambda_H). \tag{54}$$

We have seen in Subsection IV-B that the LOFDM system (φ_1, Λ_H) is optimally robust against ISI/ICI if $\tau_0 = \nu_0$. Based on Theorem IV.2 we are able now to consider more general situations.

Example 1: Assume $\tau_0 = \frac{1}{\sigma}\nu_0$ for some $\sigma > 0$ and fixed ρ. The LOFDM system that is optimally adapted to these channel conditions with respect to minimizing the joint ISI/ICI is given by $(\psi^\sigma, \Lambda_\sigma)$, where the generator matrix L_σ of Λ_σ can be computed by using Theorem IV.2 and the matching rule (24) as

$$L_\sigma = \begin{bmatrix} T & \frac{T}{2} \\ 0 & F \end{bmatrix}, \quad \text{with } T = \frac{\sqrt{2}}{\sqrt[4]{3}\sqrt{\rho\sigma}},\ F = \frac{\sqrt[4]{3}\sqrt{\sigma}}{\sqrt{2\rho}}. \tag{55}$$

The optimal pulse shape is $\psi^\sigma = \mathrm{orth}(g^\sigma, \Lambda_\sigma)$ where $\sigma = \frac{\nu_0}{\tau_0}$ by assumption.

Consider for instance $\tau_0 = \sqrt{3}\nu_0$ and $\rho = \frac{1}{2}$. By using (55) we obtain

$$L_2 = \begin{bmatrix} 2 & 1 \\ 0 & 1 \end{bmatrix} \tag{56}$$

as generator matrix of the optimal lattice Λ_2. Using (40) and (38) with L_1 as in (53) and φ_1 as in (54) we compute $\alpha = \frac{1}{\sqrt[4]{3}}$, $\beta = 0$, hence

$$\varphi_2(t) = \mathcal{F}\mathcal{D}_{\alpha^{-1}}\mathcal{C}_{-\beta\alpha^2}\mathcal{F}^{-1}\varphi_1(t) = \mathcal{F}\mathcal{D}_{\alpha^{-1}}\mathcal{F}^{-1}\varphi_1(t) = \mathcal{D}_\alpha\varphi_1(t), \tag{57}$$

where we have used the fact that $\mathcal{F}\mathcal{D}_{\alpha^{-1}} = \mathcal{D}_\alpha\mathcal{F}$. Thus the optimal LOFDM setup for the given conditions $\rho = \frac{1}{2}, \tau_0 = \sqrt{3}\nu_0$ can be schematically represented as shown in Figure 4. Analog to Figures 2 and 3 the ellipses represent $\mathrm{supp}_\varepsilon\, A(\psi_2)_{k,l}$, where we have used the same ε as in those figures.

Example 2: Assume $\rho = \frac{1}{2}$ and $\tau_0 = \sqrt{3}\nu_0$, but now let the scattering function be rotated by 45 degrees (clockwise) in the time-frequency plane, as shown in Figure 5(a). In this case Theorem IV.2 together with the adaptation rule (24) yields

$$L_2 = \begin{bmatrix} \sqrt{2} & 0 \\ 0 & \sqrt{2} \end{bmatrix} \tag{58}$$

as generator matrix of the optimal lattice Λ_2, which is a rectangular lattice in this case. Proceeding in the same way as in the previous example we calculate $\alpha = \frac{\sqrt{2}}{\sqrt[4]{3}}$, $\beta = \frac{1}{2}$, and $\varphi_2(t) = \mathcal{F}\mathcal{D}_{\alpha^{-1}}\mathcal{C}_{-\beta\alpha^2}\mathcal{F}^{-1}\varphi_1(t) = \mathcal{F}\mathcal{D}_{\alpha^{-1}}\mathcal{C}_{-\beta\alpha^2}\varphi_1(t)$. Since f_2 is the Fourier transform of a dilated chirped Gaussian, formulas (7), (8), and (23) then show that $\operatorname{supp}_\varepsilon A\varphi_2$ is (approximately) an ellipse, with ratio of semi-major vs semi-minor axis equal to $\sqrt{3}$, rotated by 45 degrees. Hence the corresponding LOFDM system (ψ, Λ_R) with $\psi = \operatorname{orth}(\varphi_2, \Lambda_R)$ can be schematically represented as in Figure 5. The ellipses in Figure 5 represent $\operatorname{supp}_\varepsilon A\psi_{k,l}$ where we have chosen the same ε as in the previous figures.

If $\nu_0 \approx 0$ then the channel is essentially frequency selective. In this case OFDM systems employing (almost) rectangular pulses such as cyclic prefix OFDM are of course optimal. The essential support of the ambiguity function of a rectangular pulse has rectangular shape.

It is clear that the optimal lattice for such pulses is a rectangular lattice. Thus the introduction of general lattices would only decrease the performance in such a situation.

V. Numerical simulations

A. *Efficient numerical implementation of LOFDM*

Before we proceed to a performance comparison between OFDM and LOFDM we briefly discuss the numerical implementation of LOFDM. We do not go into detail here, but note that the results in this paragraph can be readily derived by using the link between OFDM and Gabor analysis (see also the Appendix) and the efficient algorithms that have been developed in association with suitable finite-dimensional models for Gabor analysis [22].

The requirement for an efficient implementation puts some limits on the possible values of the entries x, y, z of the generator matrix of the lattice (cf. 29). One can easily see that an FFT-based implementation is only possible if $x, y, z \in \mathbb{Q}$. In particular if $x/y \in \mathbb{N}$ then the lattice can be written as sum of x/y rectangular lattices, which differ from each other only by the time-frequency offset. For each of these rectangular sub-lattices we can use the usual FFT-based implementation for pulse-shaping OFDM systems. An example for a "good" generator matrix is

$$L = \begin{bmatrix} T & T/2 \\ 0 & F \end{bmatrix}$$

with $TF \in \mathbb{Q}$. Specifically, if $TF = p/q$ with $p, q \in \mathbb{N}$, the length of the FFT is given by s^2pq, where s is a constant that depends on the ratio of the sampling rate and the decimation factor in the A/D conversion and is often of the form $s = 2^n$.

B. *Comparison of performance of LOFDM vs OFDM*

We compare the proposed LOFDM system to a standard pulse-shaping OFDM system of (10) associated with the rectangular lattice. Following other work on pulse shaping OFDM [6], [7], [8], [10], [5], we consider transmission systems with spectral efficiency $\rho = 0.5$ (in practice a higher spectral efficiency is certainly preferable). For both systems we use the pulse obtained from the Gaussian via $\operatorname{orth}(g^\sigma, \Lambda_R)$ and $\operatorname{orth}(g^\sigma, \Lambda_H)$ respectively. For the rectangular lattice the OFDM system obtained in that way coincides with the setup suggested in [5]. In both cases we optimally adapt the pulse and the lattice parameters to the given delay spread and Doppler spread.

For the numerical simulations we assume the channel to be wide-sense stationary with uncorrelated scattering (WSSUS), cf. [14]. We consider a Jakes-type Doppler behavior and exponential decay in the temporal direction for the scattering function [4]. In addition we assume that $\tau_0\nu_0 < 1$, i.e., the channel is underspread [14]. Zero-mean white Gaussian noise in the order of 0.2% of the signal energy is added during the simulated transmission. We choose this small percentage of noise in our comparison in order to concentrate on the effects caused by ISI and ICI.

Furthermore for a fair comparison between OFDM and LOFDM concerning their robustness against ISI/ICI, we have to exclude any additional effects resulting from coding or channel estimation. Thus we assume that the channel is known at the receiver and do not perform any coding/decoding of the data.

Recall from (13) that the received data $\tilde{c}_{k,l}$ can be written as $\tilde{c}_{k,l} = \sum_{k',l'} c_{k',l'}\langle \mathbf{H}\varphi_{k',l'}, \psi_{k,l}\rangle + \langle \varepsilon, \psi_{k,l}\rangle$.

Let $S_{\mathbf{H}}$ denote the time-varying transfer function (also known as Weyl symbol) of $\mathbf{H}$, see [14]. For underspread channels and pulse shapes that are well concentrated in time and frequency it has been shown in [8] for rectangular time-frequency lattices that

$$\langle \mathbf{H}\varphi_{k,l}, \varphi_{k,l}\rangle = S_{\mathbf{H}}(\lambda_k, \nu_l), \quad (\lambda_k, \nu_l) \in \Lambda \tag{59}$$

and that $\langle \mathbf{H}\varphi_{k',l'}, \varphi_{k,l}\rangle \approx 0$ for $k \neq k', l \neq l'$. This result also holds for general lattices. We thus can use a simple one-tap equalizer to approximately recover the data. Hence the received data can be equalized by computing

$$d_{kl} = \frac{\tilde{c}_{kl}}{S_{\mathbf{H}}(\lambda_k, \nu_l) + \sigma^2}, \tag{60}$$

where σ is the variance of the AWGN.

For both OFDM and LOFDM we compute the Signal-to-Noise-plus-Interference-Ratio (SNIR) of the transmitted data $c_{k,l}$ and the received data $d_{k,l}$ (which have been equalized according to (60)). Since both OFDM and LOFDM are orthogonal systems they are equally well (in fact optimally) adapted to AWGN. Hence any statistical difference in the SNIR can be attributed to the difference in robustness against ISI/ICI.

We fix the product $\tau_0 \cdot \nu_0$, randomly vary the parameters of the scattering for each experiment and compute the average SNIR for OFDM and LOFDM over 100 such experiments. We repeat this simulation for a variety of values $\tau_0 \cdot \nu_0$ in the range of $10^{-4} - 10^{-2}$ (but we always adapt both systems approximately optimal to the new values of τ_0 and ν_0. The result is shown in Figure 6. As expected from the theoretical analysis LOFDM yields indeed a better SNIR than OFDM. On the average the improvement of LOFDM compared to OFDM is in the range of 1dB.

VI. Extensions and final remarks

We briefly indicate some extensions and generalizations of the results presented in this paper, and discuss a few open problems.

A. Extensions to OQAM-OFDM

The pulse-shaping framework presented in Section III also applies to OQAM-OFDM. This is due to the fact that OQAM-OFDM systems can be constructed from certain OFDM systems in a similar way as Wilson bases can be constructed from certain tight Gabor frames [9]. Thus our approach shows how to design optimal pulse shapes for OQAM-OFDM for different channel conditions.

We refer to [27] for a discussion of the difficulties when one attempts to extend OQAM-OFDM systems to general time-frequency lattices.

B. OFDM vs BFDM

Recently biorthogonal frequency division multiplexing (BFDM) has been introduced [8]. The reason for considering BFDM is that by giving up the orthogonality condition one can improve the time-frequency localization of the transmitter pulse shape for $TF > 1$. This comes however at the cost of increased sensitivity to AWGN, since we no longer have an orthogonal set of transmitter functions. Nevertheless the concept of using general time-frequency lattices in order to optimally adapt the transmission functions for time-frequency dispersive channels can be applied without any modification to BFDM. We expect improvements comparable to that of LOFDM vs OFDM.

BFDM and OFDM can be seen as special cases of the following general framework which allows to fine-tune the balance between AWGN sensitivity and ISI/ICI robustness. Assume we are given a non-orthogonal linear independent set of transmission functions (h, Λ) (here h may be the Gaussian function) and let $R(h, \Lambda)$ denote the Gram matrix as defined in (31).

A pair of perfect reconstruction transmitter and receiver functions (φ, Λ), (f, Λ) can be constructed by defining

$$\varphi = \sum_{k,l} R^{-\alpha}_{k,l,0,0} h_{k,l}, \quad f = \sum_{k,l} R^{-1+\alpha}_{k,l,0,0} h_{k,l}, \quad \alpha \in [0, 1]. \tag{61}$$

Clearly the choice $\alpha = \frac{1}{2}$ leads to a standard OFDM system (with $\varphi = f$) with the pulse shape construction as used throughout the paper. The choice $\alpha = 0$ or $\alpha = 1$ corresponds to BFDM. For $0 < \alpha < 1/2$ (or $1/2 < \alpha < 1$ respectively) we obtain a transmission system that "interpolates" between OFDM and BFDM. The systems (φ, Λ) and (f, Λ) become "more and more orthogonal" as $\alpha \to \frac{1}{2}$ (the condition number of $R(\varphi, \Lambda)$ and $R(f, \Lambda)$ approaches 1), but the time-frequency localization of φ might degrade. Hence by varying α we can either put more weight on the AWGN performance or emphasize the ISI/ICI performance.

C. Modulated filterbanks, phase space packings

Modulated filter banks have attracted considerable interest in recent years see, e.g. [28], [29]. Due to the duality relations between oversampled and undersampled Gabor systems there is a nice relation between OFDM systems and paraunitary modulated filter banks. Based on this link it is clear that the pulse shape design framework as well as the use of general time-frequency lattices presented in this paper also have potential application in the construction of paraunitary modulated filter banks.

The idea of using general time-frequency lattices in connection with modulated filter banks might lead to even more significant improvement when applied to two-dimensional signals. However we do not know what the optimal lattice would be in this case. In analogy to the argument used in subsection IV-B one might speculate that the lattice that solves the sphere packing problem in $\mathbb{R}^4$ is optimal for constructing modulated filter banks for two-dimensional signals (since the corresponding phase space is now four-dimensional). However we cannot directly draw from sphere packing theory in this case, since standard sphere packing lattices are designed for $\mathbb{R}^d$, whereas in our case we are restricted to symplectic lattices. In $\mathbb{R}^2$ any lattice is symplectic, but this is no longer true in $\mathbb{R}^d$ with $d > 2$.

In fact the lattice design problem seems to lead to a new type of sphere packing problem, which one might call *Gaussian sphere packings* or *phase space packings*.

D. Some conjectures

Finally we want to state a few conjectures and observations.

For two functions f, φ we define their joint TFL as the product $\Delta\tau_f \cdot \Delta\nu_f \cdot \Delta\tau_h \cdot \Delta\nu_h$ where $\Delta\tau$ and $\Delta\nu$ are as defined in (14). If f and h are related via (61) then we conjecture that the optimal joint time-frequency localization of f and h is achieved when $\alpha = \frac{1}{2}$.

In Section III we saw that the TFL of the pulse $\psi = \text{orth}(g, \sqrt{2}, \sqrt{2})$ measured in terms of second-order moments is $(\Delta\tau_\psi \cdot \Delta\nu_\psi)^{-1} = 0.977 \cdot 4\pi$, which is believed in [5] to be the optimum among all pulses creating an OFDM system (or OQAM-OFDM system). This conjecture is plausible for rectangular lattices, but is wrong if we allow more general lattices. For instance if we use the hexagonal lattice Λ_H as defined in (28) with $T = F = \sqrt{2}$ and set $\psi_H = \text{orth}(g, \Lambda_H)$ we compute numerically $(\Delta\tau_{\psi_H} \cdot \Delta\nu_{\psi_H})^{-1} = 0.986 \cdot 4\pi$. We conjecture that this is the optimal value among all possible lattices and among all possible pulse shapes that create an LOFDM system with spectral efficiency 1/2 (and similar for other values of ρ).

It is interesting to compare the condition number of $R_R := R(g, \Lambda_R)$ with that of $R_H := R(g, \Lambda_H)$ for $T = F = \sqrt{2}$, where the generator matrices for these lattices are as defined in (27) and (28). In the first case we get $\text{cond}(R_R) = \sqrt{2}$ and in the second case $\text{cond}(R_H) \approx 1.2599$ which is suspiciously close to $\sqrt[3]{2}$. We believe that this is the minimal condition number achievable for $R(g, \Lambda)$ where Λ is any lattice of density 1/2.

VII. Appendix

In the proof of Theorem IV.2 and Theorem III.2 we make use of the link between OFDM and Gabor frames [7], [8], [9]. Recall that a general Gabor system consists of functions of the form

$$f_{m,n}(t) = e^{2\pi i \lambda_m t} f(t - \nu_n), \quad (\lambda_m, \nu_n) \in \Upsilon \tag{62}$$

where $f \in \boldsymbol{L}_2(\mathbb{R})$ is a given *window*, and Υ is a lattice in $\mathbb{R}^2$. We denote this system by (f, Υ).

We say that (f, Υ) is a *Gabor frame* for $\boldsymbol{L}_2(\mathbb{R})$ if there exist constants (*frame bounds*) $A, B > 0$ such that

$$A\|h\|^2 \le \sum_{n,m\in\mathbb{Z}} |\langle h, f_{m,n}\rangle|^2 \le B\|h\|^2, \tag{63}$$

for any $h \in \boldsymbol{L}_2(\mathbb{R})$. If $A = B$ the frame is called *tight.*

Let Y denote the generator matrix of the lattice Υ. We define the adjoint lattice Υ° as the lattice that has generator matrix $Y^\circ := \det(Y)^{-1} Y$.

There is a deep and elegant *duality relation* between Gabor frames and Gabor Riesz bases which can be stated as follows [30], [31], [32].

Theorem VII.1: (f, Υ) is a Riesz basis (orthogonal basis) for its closed linear span if and only if (f, Υ°) is a frame (tight frame) for $\boldsymbol{L}_2(\mathbb{R})$.

It is interesting to note that this duality relation can already be extracted from a paper of Rieffel on non-commutative tori [33].

Proof of Theorem III.2:

By the orthogonality relations of the ambiguity function (e.g., see Chapter 4.2 in [12]) we have that $\|Af - A\varphi\| = \|f - \varphi\|^2$. Now (22) follows immediately from Theorem 2.1 in [34] by using the duality relations between the systems (f, T, F) and $(f, 1/F, 1/T)$.

To show part (ii) we once more use the duality relations. We can write ψ as $\psi = \sqrt{TF} S^{-\frac{1}{2}} f$ where S is the Gabor frame operator of the frame $(f, 1/F, 1/T)$ (the normalization by $\sqrt{TF}$ yields $\|\psi\| = 1$). There holds $\theta_{\min} \le \frac{1}{TF} S \le \theta_{\max}$, see Theorem 3.1 in [30]. The estimate (23) follows from the calculation

$$\|f - \psi\| = \|(I - \sqrt{TF} S^{-\frac{1}{2}}) f\| \le \|I - \sqrt{TF} S^{-\frac{1}{2}}\|_{op} \le \max\left\{|1 - 1/\sqrt{\theta_{\min}}|, |1 - 1/\sqrt{\theta_{\max}}|\right\}, \tag{64}$$

where we have used the Spectral Mapping Theorem in the last step of (64).

❏

Acknowledgments

We are grateful to Greg Kuperberg for many interesting discussions on sphere packings. We also want to thank Werner Kozek as well as Franz Hlawatsch and his co-workers for their Matlab channel simulation files.

References

[1] W. Y. Zou and Y. Wu, "COFDM: An overview," *IEEE Trans. Broadc.*, vol. 41, no. 1, pp. 1–8, March 1995.

[2] D. Castelain, B. Le Floch, and R. Halbert-Lassalle, "Digital sound broadcasting to mobile receivers," *IEEE Trans. Consumer Electron.*, vol. 73, pp. 30–34, 1989.

[3] A. S. Macedo and E. S. Sousa, "Coded OFDM for broadband indoor wireless systems," in *Proc. IEEE Int. Conf. Communications (ICC)*, Montreal (Canada), 1997.

[4] T. S. Rappaport, *Wireless communications: Principles & Practice*, Prentice Hall, New Jersey, 1996.

[5] B. Le Floch, M. Alard, and C. Berrou, "Coded orthogonal frequency division multiplex," *Proc. of IEEE*, vol. 83, no. 6, pp. 982–996, June 1995.

[6] A. Vahlin and N. Holte, "Optimal finite duration pulses for OFDM," *IEEE Trans. Comm.*, vol. 44, no. 1, pp. 10–14, 1995.

[7] R. Haas and J.-C. Belfiore, "A time–frequency well–localized pulse for multiple carrier transmission," *Wireless Personal Communications*, vol. 5, pp. 1–18, 1997.

[8] W. Kozek and A. Molisch, "Nonorthogonal pulseshapes for multicarrier communications in doubly dispersive channels," *IEEE J. Sel. Areas Comm.*, vol. 16, no. 8, pp. 1579–1589, 1998.

[9] H. Bölcskei, "Orthogonal frequency division multiplexing based on offset QAM," in *Advances in Gabor Analysis*, H. G. Feichtinger and T. Strohmer, Eds., chapter 12. Birkhäuser, Boston, MA, 2002.

[10] H. Bölcskei, P. Duhamel, and R. Hleiss, "Efficient design of OFDM/OQAM pulse shaping filters," *IEEE Trans. Comm.*, 2000, submitted.

[11] T. Strohmer, "Approximation of dual Gabor frames, window decay, and wireless communications," *Appl. Comp. Harm. Anal.*, vol. 11, no. 2, pp. 243–262, 2001.

[12] O. Christensen, *An introduction to frames and Riesz bases*, Birkhäuser, Boston, 2003.

[13] R. Young, *An Introduction to Nonharmonic Fourier Series*, Academic Press, New York, 1980.

[14] P.A. Bello, "Characterization of randomly time–variant linear channels," *IEEE Trans. Comm. Syst.*, vol. 11, pp. 360–393, 1963.

[15] I. Daubechies, *Ten Lectures on Wavelets*, CBMS-NSF Reg. Conf. Series in Applied Math. SIAM, 1992.

[16] A.J.E.M. Janssen, "The duality condition for Weyl-Heisenberg frames," in *Gabor Analysis and Algorithms: Theory and Applications*, H.G. Feichtinger and T. Strohmer, Eds., chapter 1, pp. 33–84. Birkhäuser, Boston, 1998.

[17] L. Cohen, "The uncertainty principle for the short-time fourier transform and wavelet transform," in *Wavelet Transforms and Time-Frequency Signal Analysis*, L. Debnath, Ed., chapter 8. Birkhäuser, Boston (MA), 2001.

[18] A. Bonami, B. Demange, and P. Jaming, "Hermite functions and Uncertainty principles for the Fourier and the Windowed Fourier transforms," preprint, 2001.

[19] H. Bölcskei and A.J.E.M. Janssen, "Gabor frames, unimodularity, and window decay," *J. Four. Anal. Appl.*, vol. 6, no. 3, pp. 255–276, 2000.

[20] H.G. Feichtinger and G. Zimmermann, "A space of test functions for Gabor analysis," in *Gabor Analysis and Algorithms: Theory and Applications*, H.G. Feichtinger and T. Strohmer, Eds., chapter 3, pp. 123–170. Birkhäuser, Boston, 1998.

[21] A.J.E.M. Janssen, "personal communication," 1998.

[22] T. Strohmer, "Numerical algorithms for discrete Gabor expansions," in *Gabor Analysis and Algorithms: Theory and Applications*, H.G. Feichtinger and T. Strohmer, Eds., chapter 8, pp. 267–294. Birkhäuser, Boston, 1998.

[23] W. Kozek, "Adaptation of Weyl–Heisenberg frames to underspread environments," in *Gabor Analysis and Algorithms: Theory and Applications*, H.G. Feichtinger and T. Strohmer, Eds., chapter 10, pp. 323–352. Birkhäuser, Boston, 1998.

[24] J.H. Conway and N.J.A. Sloane, Eds., *Sphere Packings, Lattices and Groups*, Grundlehren der mathematischen Wissenschaften. Springer Verlag, New York, Berlin, Heidelberg, 1993.

[25] G.B. Folland, *Harmonic Analysis in Phase Space*, Annals of Math. Studies. Princeton Univ. Press, Princeton (NJ), 1989.

[26] S. Barbarossa and R. Torti, "Chirped-OFDM for transmissions over time-varying channels with linear delay/Doppler spreading," in *Proc. IEEE ICASSP-01*, Salt Lake City, Utah, 2001, vol. 4, pp. 2377–2380.

[27] G. Kutyniok and T. Strohmer, "On the (non-)existence of Wilson bases for general time-frequency lattices," 2002, manuscript.

[28] Z. Cvetkovic and M. Vetterli, "Oversampled filter banks," *IEEE Trans. Signal Proc.*, vol. 46, no. 5, pp. 1245–1255, 1998.

[29] H. Bölcskei and F. Hlawatsch, "Oversampled modulated filter banks," in *Gabor Analysis and Algorithms: Theory and Applications*, H.G. Feichtinger and T. Strohmer, Eds., chapter 9, pp. 295–322. Birkhäuser, Boston, 1998.

[30] A.J.E.M. Janssen, "Duality and biorthogonality for Weyl-Heisenberg frames," *J. Four. Anal. Appl.*, vol. 1, no. 4, pp. 403–436, 1995.

[31] I. Daubechies, H. Landau, and Z. Landau, "Gabor time-frequency lattices and the Wexler-Raz identity," *J. Four. Anal. Appl.*, vol. 1, no. 4, pp. 437–478, 1995.

[32] Amos Ron and Zuowei Shen, "Weyl-Heisenberg frames and Riesz bases in $L_2(\mathbf{R}^d)$," *Duke Math. J.*, vol. 89, no. 2, pp. 237–282, 1997.

[33] M.A. Rieffel, “Projective modules over higher-dimensional noncommutative tori,” *Canad. J. Math.*, vol. 40, no. 2, pp. 257–338, 1988.

[34] A.J.E.M. Janssen and T. Strohmer, “Characterization and computation of canonical tight windows for Gabor frames,” *J. Four. Anal. Appl.*, vol. 8, no. 1, pp. 1–28, 2002.

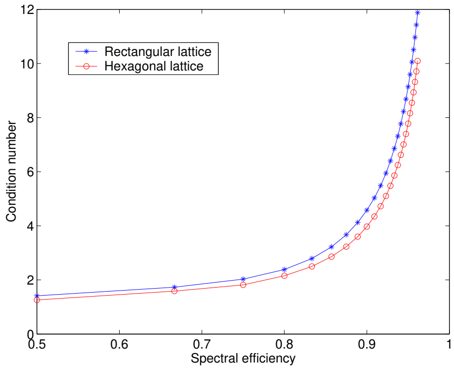

Fig. 1. Comparison of the condition number of the Gram matrix of the OFDM-type function system (g^σ, T, F) (g^σ is the Gaussian) for the rectangular lattice and the hexagonal lattice when the product $(TF)^{-1}$ approaches 1. In both cases the condition number is small for $TF \in [\frac{1}{2}, \frac{4}{5}]$. As expected cond$(R)$ for the hexagonal lattice is definitely smaller than cond(R) for the rectangular lattice, thus demonstrating the potential advantage of designing OFDM systems for general time-frequency lattices.

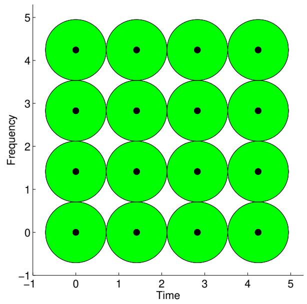

Fig. 2. An OFDM system with rectangular lattice in the time-frequency plane. The data symbols $c_{k,l}$ are transmitted at the lattice points (kT, lF). The spheres represent the effective support $\mathrm{supp}_\varepsilon\, A\psi_{k,l}$ of the ambiguity function $A\psi_{k,l}$. The choice of ε is such that the difference to the LOFDM setup displayed in Figure 3 becomes obvious.

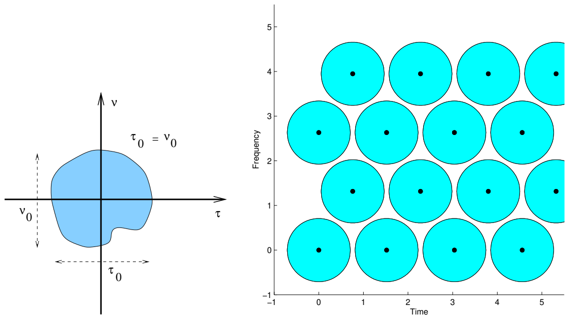

(a) (b)

Fig. 3. Optimal LOFDM system (Fig. 3(b)) for the channel scattering shown in Fig. 3(a). The data symbols $c_{k,l}$ are transmitted at hexagonal lattice points. The gray spheres represent $\mathrm{supp}_\varepsilon\, A\psi_{k,l}$ with the same ε as in Figure 2. The use of the hexagonal lattice clearly increases the distance between adjacent spheres as compared to the rectangular lattice (cf. Figure 2), thus leading to reduced ISI/ICI for time-frequency dispersive channels.

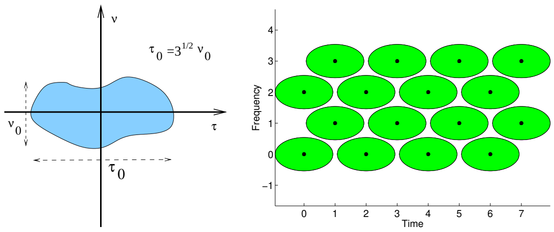

(a) (b)

Fig. 4. Optimal LOFDM setup (Fig. 4(b)) for a wireless channel with $\tau_0 = \sqrt{3}\nu_0$ (scattering function shown in Fig. 4(a)). The ellipses represent $\mathrm{supp}_\varepsilon\, A(\psi_2)_{k,l}$, where we have chosen the same ε as in Figure 3.

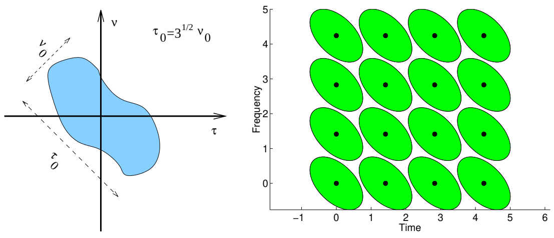

(a) (b)

Fig. 5. Optimal LOFDM setup (Fig. 5(b)) for a wireless channel with 45-degree rotated scattering function satisfying $\tau_0 = \sqrt{3}\nu_0$ (see Fig. 5(a)). The ellipses represent $\operatorname{supp}_\varepsilon A(\psi_2)_{k,l}$, where we have chosen the same ε as in Figure 3.

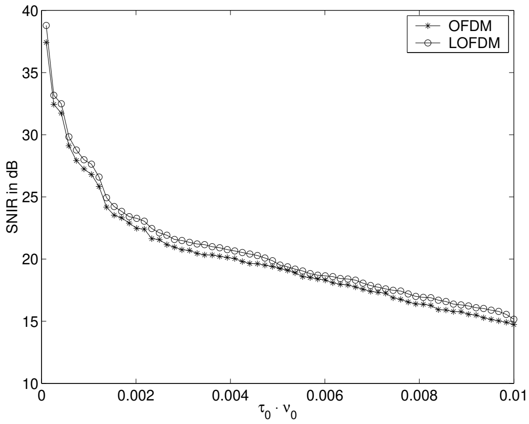

Fig. 6. Comparison of Signal to Noise-plus-Interference Ratio (SNIR) for OFDM and LOFDM for $\tau_0 \cdot \nu_0 \in [10^{-4}, 10^{-2}]$. The proposed LOFDM scheme yields an improvement of about 1dB.